A rapid hydrothermal synthesis of rutile SnO$_2$ nanowires

O. Lupan [a,b,*], L. Chow [a], G. Chai [c], A. Schulte [a], S. Park [a], H. Heinrich [a,d]

[a] *Department of Physics, University of Central Florida, PO Box 162385, Orlando, FL 32816-2385, USA*
[b] *Department of Microelectronics and Semiconductor Devices, Technical University of Moldova, Stefan cel Mare Blvd. 168, Chisinau MD-2004, Republic of Moldova*
[c] *Apollo Technologies, Inc. 205 Waymont Court, S111, Lake Mary, FL 32746, USA*
[d] *Advanced Materials Processing and Analysis Center, and Department of Mechanical, Materials, and Aerospace Engineering, University of Central Florida, Orlando, FL 32816, USA*

ARTICLE INFO

ABSTRACT

Tin oxide (SnO$_2$) nanowires with rutile structure have been synthesized by a facile hydrothermal method at 98 °C. The morphologies and structural properties of the as-grown nanowires/nanoneedles were characterized by scanning electron microscopy (SEM), transmission electron microscopy (TEM), selected area electron diffraction, X-ray diffraction and Raman spectroscopy. The SEM images reveal tetragonal nanowires of about 10–100 μm in length and 50–100 nm in radius. The Raman scattering peaks indicate a typical rutile phase of the SnO$_2$. The effects of molar ratio of SnCl$_4$ to NH$_4$OH on the growth mechanism are discussed.

© 2009 Elsevier B.V. All rights reserved.

1. Introduction

A new generation of one-dimensional (1D) nanoarchitectures, such as nanowires, nanorods and nanoneedles has been produced and attracted considerable attention in the materials research community [1]. The interest is motivated by the physical and chemical properties, which are highly dependent on the aspect ratio and shape [1,2]. Extensive efforts have been made on developing new methods to synthesize, manipulate and tailoring functionalities of a variety of 1D nanostructured materials (SnO$_2$, ZnO, CdS, In$_2$O$_3$, etc.) [1–3]. Among them, rutile SnO$_2$, an n-type semiconductor with a wide band gap (Eg = 3.62 eV at 300 K), and excellent optical and electrical properties, is a strategic material for a range of technological applications [4]. Its practical uses include ultrasensitive gas sensors [5], optoelectronic devices [6], electrodes for solar cells [4] and anode material for lithium batteries [7].

SnO$_2$ nanoarchitectures have been synthesized by the self-catalytic vapor–liquid–solid (VLS) method [6], calcination process [7], chemical vapor deposition [8], thermal evaporation [1], hydrothermal [9], laser ablation technique [10], solvothermal [11] and carbothermal reduction [12]. These techniques all require a growth temperature of 900 °C or higher, which makes them difficult for certain device applications and which are often difficult

to control reproducibly [13]. Guo et al. [14] has reported a low-temperature hydrothermal synthesis of SnO$_2$ nanorods at 160 °C, but the process requires at least 12 h. Vayssieres and Graetzel [15] reported SnO$_2$ nanorods arrays grown on F-SnO$_2$ glass substrates by aqueous thermohydrolysis at 95 °C.

This paper presents an inexpensive and rapid fabrication technique for one-dimensional (1D) tin oxide (SnO$_2$) nanowires with rutile structure synthesized by a facile hydrothermal method at 95–98 °C for 15 min. It permits rapid and controlled growth of tin oxide nanowires without the use of templates or seeds. The obtained tin oxide nanowires are distributed on the surface of Si/SiO$_2$ substrates and individual nanowires can be easily transferred to other substrates which are decisive factor for single nanowire ultrasensitive sensors fabrication.

Our technique is faster and cost-effective, which is important for large scale applications in nanoelectronics/nanotechnologies and can find a wide range of applications.

2. Experimental

Rutile-structured SnO$_2$ nanowires/nanoneedles were synthesized at a low temperature by a hydrothermal method without any other seeds, templates or surfactant. A solution containing tin chloride [SnCl$_4$·5H$_2$O, 0.01–0.03 M] (purity 99.5%) and ammonia [NH$_4$(OH), 29.5%] (Fisher Scientific) was employed for growth of tin oxide nanowires and nanoneedles. Both reagents were used in the received form without further purification. A hydrothermal reactor [3] with a cap was filled with aqueous solution. In a typical procedure, Si wafers and glass substrates were cleaned according to

* Corresponding author at: Department of Physics, University of Central Florida, PO Box 162385, Orlando, FL 32816-2385, USA. Tel.: +1 407 823 2333; fax: +1 407 823 5112.
E-mail addresses: lupan@physics.ucf.edu, lupanoleg@yahoo.com (O. Lupan).
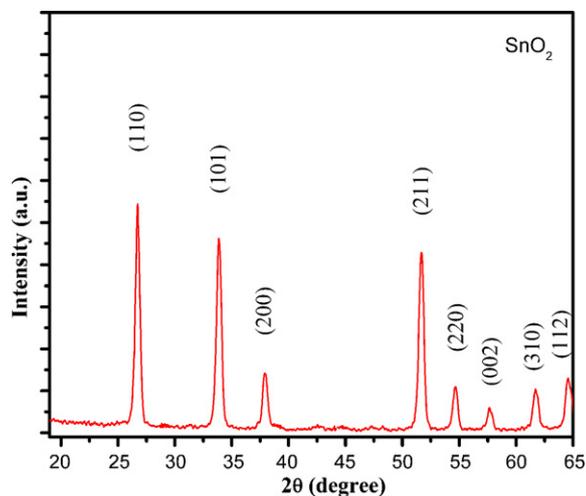
Fig. 1. XRD pattern of the SnO$_2$ nanowires prepared through the hydrothermal reaction on a SiO$_2$/Si substrate.

previous work [16]. Subsequently, a piece of cleaned Si substrate was placed in the reactor and healed at a temperature 95–98 °C for 15 min on a hot plate [3]. Then the reactor was allowed to cool down. Finally, the SnO$_2$ nanowires were thoroughly washed with deionized water to eliminate residual unreacted species and the reaction byproduct, and annealed at 370 °C for 5 min.

A scanning electron microscope (SEM, JEOL 6400F) was used to observe the SnO$_2$ nanowires using an operating voltage of 10 kV. The obtained samples were characterized by X-ray powder diffraction (XRD) using a Rigaku 'D/B max' X-ray diffractometer with Cu Kα radiation (λ = 1.54178 Å) operating at 40 kV and 30 mA. Transmission electron microscopy (TEM) of the samples was performed with a FEI Tecnai F30 transmission electron microscope operated at an accelerating voltage of 300 kV. For the TEM observation, the samples were collected on a carbon holey grid. The composition was characterized by Energy Dispersion X-ray Spectroscopy (EDX) in SEM and TEM. Micro-Raman measurements were performed on a Horiba Jobin Yvon LabRam IR system at a spatial resolution of 2 μm. Raman scattering was excited with the 633 nm line of a He–Ne laser with output power less than 4 mW at the sample.

3. Results and discussion

Fig. 1 shows the XRD patterns from the synthesized SnO$_2$ samples which demonstrates the SnO$_2$ tetragonal rutile structure with lattice constants $a = b = 0.4743$ nm and $c = 0.3186$ nm, which match well with the standard XRD data file of SnO$_2$ (JCPDS-041-1445) (ICSD data) [17]. The peaks were sharp indicating high crystallinity of SnO$_2$ nanowires.

Fig. 2(a) and (b) shows the detailed morphologies of the SnO$_2$ nanowires prepared through the hydrothermal reaction. The nanowires/nanoneedles have a uniform length of about 10–20 μm and diameters of about 0.1 μm (Fig. 2a) grown by using precursor with the ratio between SnCl$_4$ and NH$_4$OH as (1:25).

The morphology of nanowires was found to be dependent on the synthesis conditions. The dimensions and aspect ratio are a function of growth time, temperature and Sn^{4+}/OH$^-$ ratio in solution. Thus, by this method, we also synthesized SnO$_2$ thinner nanowires (Fig. 2a) by decreasing the concentration of SnCl$_4$ in solution. Fig. 2b shows the morphology of SnO$_2$ nanowires synthesized at 95 °C on a SiO$_2$/Si substrate synthesized according to technology reported previously [3]. The nanowires with larger radius were synthesized by using precursor with the ratio between SnCl$_4$ and NH$_4$OH of (1:20) (Fig. 2b). In the inset of Fig. 2b the end planes of the SnO$_2$ nanowires clearly reflect the tetragonal symmetry. The products consisted of nanowires as well as nanoparticles. The diameters of tin oxide nanowires are in the range of 70–150 nm with lengths of the order of 20–100 μm.

When the ratio between SnCl$_4$ and NH$_4$OH is as high as 1:20 we obtain long tetragonal square-based nanowires. Experiment results showed that the molar ratio of (1:20) made the hydrolysis occur rapidly due to of higher quantity of nuclei. By further increasing the ratio above 1:30 no products is formed and we have only solution. This can be explained by the fact that the quantity of nuclei depends on the precursor concentration and by increasing OH$^-$ ion concentration means the decreasing Sn^{4+} ion concentration (the total volume of solution is fixed). Therefore, SnO$_2$ nanowires growth dependent on the degree of supersaturation and Sn^{4+}, served as the precursor in reverse micelle. Thus at higher OH$^-$ ion concentration growth of nanowires do not take place.

The transmission electron microscopy (TEM) image in Fig. 3 shows the tin oxide nanowires/nanoneedles which were synthesized. The TEM images indicate that the entire as-grown nanowires are single-crystalline SnO$_2$ with a rutile structure grown along the [1 0 1] direction, which is consistent with the XRD results. The HRTEM lattice fringes and SAED patterns shown in Fig. 3 reveal that, in this region, the nanowires possess a single-crystalline structure. Typical selected-area electron diffraction (SAED) pattern (Fig. 3), indicates that the nanowires are good quality with rutile SnO$_2$ structure. According to the SAED pattern taken, the growth direction of tin oxide nanowires is along [1 0 1] direction. This is in agreement with previous reports [18].
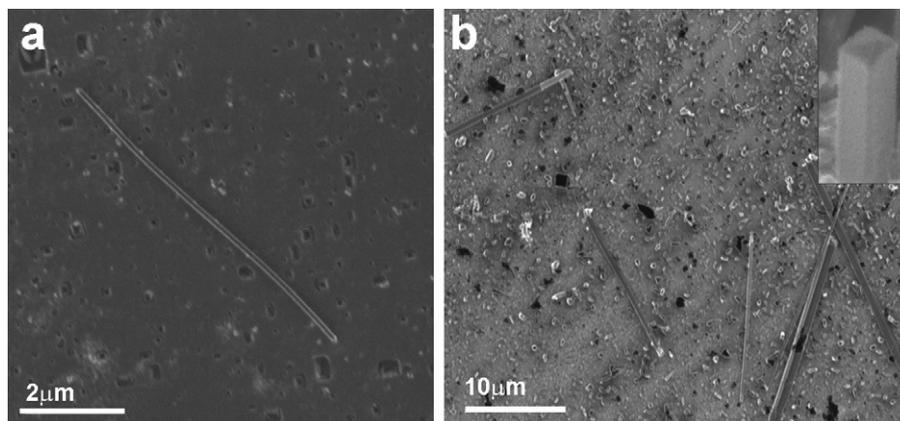
Fig. 2. Scanning electron micrographs of hydrothermally grown (a) SnO$_2$ nanowires on a SiO$_2$/Si substrate; (b) SnO$_2$ nanowires/nanoneedles on a SiO$_2$/Si substrate. The inset is a magnified image of the end planes of the tetragonal SnO$_2$ nanowires.
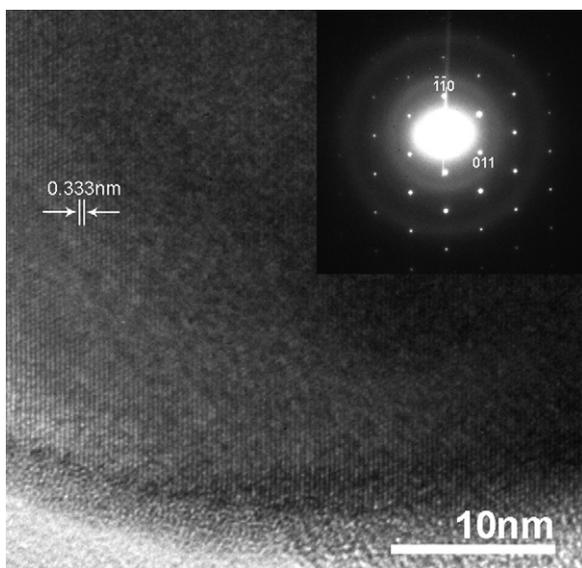
Fig. 3. HRTEM images of an individual SnO_2 nanowire. The upper right inset is a SAED of a single-crystalline SnO_2 nanowire.

In order to study the local structure of tin oxide samples we employed Raman spectroscopy at room temperature to study effects of crystal structure, defects and structural disorder in SnO_2 nanowires/nanoneedles.

The rutile structure SnO_2 belongs to the point group D_{4h}^{14} and space group p_4/mnm [21–23] with tin and oxygen atoms in a 2a and 4f positions, respectively. On the basis of group theory [23] the normal lattice vibration at the Γ point of the Brillouin zone is as follows [24]:

$$\Gamma = \Gamma_1^+(1A_{1g}) + \Gamma_2^+(1A_{2g}) + \Gamma_3^+(1B_{1g}) + \Gamma_4^+(1B_{2g}) + \Gamma_5^-(1E_g)$$
$$+ \Gamma_1^-(1A_{2u}) + 2\Gamma_4^-(B_{1u}) + 3\Gamma_5^+(E_u) \qquad (1)$$

The Raman active modes are B_{1g}, E_g, A_{1g}, and B_{2g}. In these modes the oxygen atoms vibrate while the Sn atoms are at rest. The E_g, mode represents vibrations with displacements in the direction of the c-axis, but A_{1g}, and B_{1g}, are vibrations with displacements in directions perpendicular to the c-axis [25]. Seven modes of A_{2u}, and $3E_u$, are infrared (IR) active and two modes of A_{2g}, and B_{1u}, are inactive [23].

Fig. 4 shows the Raman spectra of the nanowires in the wavenumber range (300–850 cm^{-1}). Raman spectra of SnO_2 films and single crystals have been extensively studied and reported
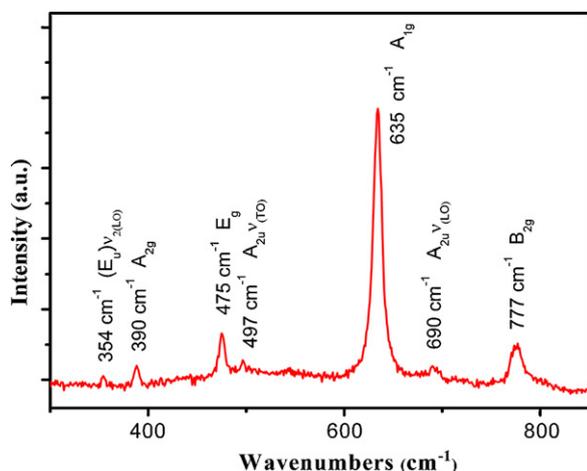
Fig. 4. Micro-Raman scattering spectra of the rutile tin oxide nanowires.

[19–26]. However, for nanowires the surface atoms represent a non-negligible fraction of atoms [24] and may cause specific spectral changes. In our samples there are Raman peaks at 354, 390, 475, 497, 635, 690, and 777 cm^{-1} in the Raman spectra (Fig. 4), which are in agreement with those of a rutile SnO_2 single crystal [19–25]. This is in agreement with the results of group-theory analysis [20,21]. These peaks are attributed to the $(E_u)V_{2(LO)}$, A_{2g}, E_g, $(A_{2u})V_{(TO)}$, A_{1g}, $(A_{2u})V_{(LO)}$, and B_{2g}, vibrational modes of SnO_2 [22–25].

The A_{1g} mode at 635 cm^{-1} in Fig. 4 showed line broadening due to finite size of the diameter ($\sim$100 nm) of nanoneedle (nanowire), which is in accordance with previous report [26].

In Fig. 4 the dominant peak (635 cm^{-1}) is assigned to the A_{1g}, vibrational mode of the SnO_2 crystal. This band is sensitive to the size [21]. A red shift for A_{1g}, was observed in our experiments with decrease of SnO_2 nanocrystal size. From the morphological investigation and the structural characterization of nanowires, we propose the following growth mechanism.

The molar ratio of Sn^{4+} to OH^- was found to be an important parameter that influences the tin oxide nanomaterial morphology. At lower ratios we obtained only irregular nano/microparticles. We observed that the aspect ratio of as-prepared SnO_2 nanowires as the molar ratio of $SnCl_4$ to NH_4OH varies from 1:10 to 1:30 (Fig. 2a and b), which is in agreement with previous reports [27,28].

The growth of SnO_2 nanowires occurs according to the following reaction [27,28]:

$$NH_4OH \leftrightarrow NH_3 + H_2O \qquad (2)$$

$$2H_2O \Leftrightarrow H_3O^+ + OH^-, K_w = 10^{-14} \text{ion-product constant} \qquad (3)$$
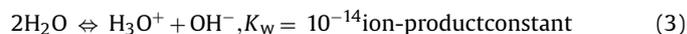
At the beginning a higher Sn^{4+}, ion concentration accelerates the nucleation process [28] and nuclei are formed:

$$Sn^{4+} + 4OH^- \rightarrow SnO_2 + 2H_2 \qquad (4)$$

$$Sn^{4+} + 4OH^- \rightarrow Sn(OH)_4 \qquad (5)$$

$$Sn^{4+} + 6OH^- \rightarrow (Sn(OH)_6)^{2-} \qquad (6)$$

The amphoteric hydroxide $Sn(OH)_4$ dissolves in ammonia solution and forms $Sn(OH)_6^{2-}$ anions.

$$Sn(OH)_4 \xrightarrow{\text{hydrothermal condition}} SnO_2 + 2H_2O \qquad (7)$$

$$(Sn(OH)_6)^{2-} \xrightarrow{\text{hydrothermal condition}} SnO_2 + 2H_2O + 2OH^- \qquad (8)$$
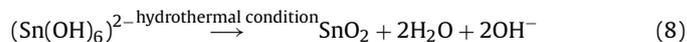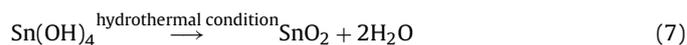
The concentration of tin ions in solution is of influencing to the diameter of nanowires. We found that the molar ratio of Sn^{4+}, to OH^-, ions for the optimal growth of elongated SnO_2 nanowires is 1:20–25.

4. Conclusion

In summary, a rapid hydrothermal method was developed to synthesize long SnO_2 nanowires at low temperature for 15–20 min.

We investigated the synthesis of SnO_2 nanowires/nanoneedles by a low-temperature (95–98 °C) hydrothermal method. The as-grown SnO_2 nanowires have diameters of 50–150 nm and lengths of 10–100 μm. The individual straight nanowires have a rectangular cross-section.

The Raman spectra and XRD pattern demonstrate that the nanowires are single-crystalline tin oxide with rutile structure. The shift of Raman peaks to a lower frequency can be associated with the size effect in nanowires.

The growth mechanism of SnO_2 nanowires is also discussed. The technique reported here could open new applications of SnO_2 nanowires, especially for ultrasensitive gas nanosensors [29] and nanodevices fabrication [30,31,32]. Further work on optimization of the synthesis conditions such as heating rate and duration to control the aspect ratio of the nanowires is underway.

Acknowledgements

References

[1] Z.W. Pan, Z.R. Dai, Z.L. Wang, Science 291 (2001) 1947.
[2] A.P. Alivisatos, Science 271 (1996) 933.
[3] O. Lupan, L. Chow, G. Chai, B. Roldan, A. Naitabdi, A. Schulte, Mater. Sci. Eng. B 145 (2007) 57.
[4] B. Liu, H.C. Zeng, J. Phys. Chem. B 108 (2004) 5867.
[5] G. Sberveglieri, C. Baratto, E. Comini, G. Faglia, M. Ferroni, A. Ponzoni, A. Vomiero, Sens. Actuators B 121 (2007) 208.
[6] Y.Q. Chen, X.F. Cui, K. Zhang, D.Y. Pan, S.Y. Zhang, B. Wang, J.G. Hou, Chem. Phys. Lett. 369 (2003) 16.
[7] M. Li, Q. Lu, Y. Nuli, X. Qian, Electrochem. Solid-State Lett. 10 (8) (2007) K33–K37.
[8] D. Calestani, M. Zha, A. Zappettini, L. Lazzarini, G. Salviati, L. Zanotti, G. Sberveglieri, Mater. Sci. Eng. C 25 (2005) 625.
[9] O. Lupan, L. Chow, G. Chai, H. Heinrich, S. Park, A. Schulte, J. Cryst. Growth 311 (2008) 152.
[10] Z.Q. Liu, D.H. Zhang, S. Han, C. Li, T. Tang, W. Jin, X.L. Liu, B. Lei, C.W. Zhou, Adv. Mater. 15 (2003) 1754.
[11] G. Cheng, K. Wu, P. Zhao, Y. Cheng, X. He, K. Huang, J. Cryst. Growth 309 (2007) 53.
[12] J.X. Wang, D.F. Liu, X.Q. Yan, H.J. Yuan, L.J. Ci, Z.P. Zhou, Y. Gao, L. Song, L.F. Liu, W.Y. Zhou, G. Wang, S.S. Xie, Solid State Commun. 130 (2004) 89.
[13] S. Budak, G.X. Miao, M. Ozdemir, K.B. Chetry, A. Gupta, J. Cryst. Growth 291 (2006) 405.
[14] C. Guo, M. Cao, C. Hu, Inorg. Chem. Commun. 7 (2004) 929.
[15] L. Vayssieres, M. Graetzel, Angew. Chem. Int. Ed. 43 (28) (2004) 3666.
[16] O.I. Lupan, S.T. Shishiyanu, L. Chow, T.S. Shishiyanu, Thin Solid Films 516 (2008) 3338.
[17] Joint Committee on Powder Diffraction Standards, Powder Diffraction File No. JCPDS-41-1445) (ICSD data).
[18] Z.R. Dai, Z.W. Pan, Z.L. Wang, Adv. Funct. Mater. 13 (2003) 9.
[19] J.F. Scott, J. Chem. Phys. 53 (1970) 852.
[20] H. Kohno, T. Iwasaki, Y. Mita, S. Takeda, J. Appl. Phys. 91 (2002) 3232.
[21] V.G. Kravets, Opt. Spectrosc. 103 (2007) 766.
[22] P.S. Peercy, B. Morosin, Phys. Rev. B 7 (1973) 2779.
[23] J.G. Traylor, H.G. Smith, R.M. Nicklow, M.K. Wilkinson, Phys. Rev. B 3 (1971) 3457.
[24] Z.W. Chen, J.K.L. Lai, C.H. Shek, Phys. Rev. B 70 (2004) 165314.
[25] R.S. Katiyars, P. Dawsons, M.M. Hargreaves, G.R. Wilkinson, J. Phys. C: Solid State Phys. 4 (1971) 2421.
[26] A. Dieguez, A. Romano-Rodriguez, A. Vila, J.R. Morante, J. Appl. Phys. 90 (2001) 1550.
[27] J. Zhang, L.D. Sun, J.L. Yin, H.L. Su, C.S. Liao, C.H. Yan, Chem. Mater. 14 (2002) 4172.
[28] D.F. Zhang, L.D. Sun, J.L. Yin, C.H. Yan, Adv. Mater. 15 (2003) 1022.
[29] F. Hernández-Ramírez, A. Tarancón, O. Casals, J. Arbiol, A. Romano-Rodríguez, J.R. Morante, Sens. Actuators B 121 (2007) 3.
[30] O. Lupan, G. Chai, L. Chow, Microelectr. J. 38 (12) (2007) 1211.
[31] O. Lupan, G. Chai, L. Chow, Microelectr. Eng. 85 (11) (2008) 2220.
[32] O. Lupan, L. Chow, G. Chai, L. Chernyaka, O. Lopatiuk-Tirpaka, H. Heinrich, Physica Status Solidi (a) 205 (2008) 2673.